Research Square

Preprints are preliminary reports that have not undergone peer review.
They should not be considered conclusive, used to inform clinical practice,
or referenced by the media as validated information.

Diffusion tractography of the olfactory pathway and odor recognition

Daiki Sasabayashi

ds179@med.u-toyama.ac.jp

Harvard Medical School

Yogesh Rathi

Harvard Medical School

Jon Haitz Legarreta

Harvard Medical School

Kazutoshi Kitajima

Harvard Medical School

Hazem Iaali

Harvard Medical School

Hiroko Itoh

University of Toyama Graduate School of Medicine and Pharmaceutical Sciences

Haruko Tachibana

University of Toyama Graduate School of Medicine and Pharmaceutical Sciences

Yuko Higuchi

University of Toyama Graduate School of Medicine and Pharmaceutical Sciences

Kyo Noguchi

University of Toyama Graduate School of Medicine and Pharmaceutical Sciences

Shinsuke Koike

The University of Tokyo Institute for Diversity and Adaptation of Human Mind

Yoji Hirano

University of Miyazaki

Martha E. Shenton

Harvard Medical School

Nikos Makris

Boston University

Tsutomu Takahashi

University of Toyama Graduate School of Medicine and Pharmaceutical Sciences

Marek Kubicki

Harvard Medical School

Richard J Rushmore

Boston University

Research Article

Keywords: Olfactory pathway, Olfactory function, Tractography, White matter, Diffusion imaging

Posted Date: November 19th, 2026

DOI: https://doi.org/10.21203/rs.3.rs-11481263/v1

License: This work is licensed under a Creative Commons Attribution 4.0 International License.
Read Full License

Additional Declarations: No competing interests reported.

Diffusion tractography of the olfactory pathway and odor recognition

Daiki Sasabayashi[1,2,3*], Yogesh Rathi[1,4,5], Jon Haitz Legarreta[5,6], Kazutoshi Kitajima[1,7], Hazem Iaali[1], Hiroko Itoh[2,3], Haruko Tachibana[2,3], Yuko Higuchi[2,3], Kyo Noguchi[8], Shinsuke Koike[9,10,11,12], Yoji Hirano[13,14], Martha E. Shenton[1,4,5], Nikos Makris[1,15,16], Tsutomu Takahashi[2,3], Marek Kubicki[1,4,5] and Richard J Rushmore[1,15,16]

[1]Psychiatry Neuroimaging Laboratory, Department of Psychiatry, Brigham and Women's Hospital, Harvard Medical School, Boston, MA, USA

[2]Department of Neuropsychiatry, University of Toyama Graduate School of Medicine and Pharmaceutical Sciences, Toyama, Japan

[3]Research Center for Idling Brain Science, University of Toyama, Toyama, Japan

[4]Department of Psychiatry, Massachusetts General Hospital, Harvard Medical School, Boston, MA, USA

[5]Department of Radiology, Brigham and Women's Hospital, Harvard Medical School, Boston, MA, USA

[6]Harvard Medical School, Boston, MA, USA

[7]Department of Neuropsychiatry, Graduate School of Medical Sciences, Kyushu University, Fukuoka, Japan

[8]Department of Radiology, University of Toyama Graduate School of Medicine and Pharmaceutical Sciences, Toyama, Japan

[9]The University of Tokyo Institute for Diversity and Adaptation of Human Mind,

Tokyo, Japan

[10]Center for Evolutionary Cognitive Sciences, Graduate School of Art and Sciences, The University of Tokyo, Tokyo, Japan

[11]International Research Center for Neurointelligence, The University of Tokyo Institutes for Advanced Study, The University of Tokyo, Tokyo, Japan

[12]Department of Child Neuropsychiatry, Graduate School of Medicine, The University of Tokyo, Hongo 7-3-1, Bunkyo-ku, Tokyo 113-8655, Japan

[13]Department of Psychiatry, Faculty of Medicine, Division of Clinical Neuroscience, University of Miyazaki, Miyazaki, Japan

[14]Institute of Industrial Science, The University of Tokyo, Tokyo, Japan

[15]Department of Anatomy and Neurobiology, Chobanian and Avedisian School of Medicine, Boston University, Boston, MA, USA

[16]Center for Morphometric Analysis, Department of Neurology and Psychiatry, Massachusetts General Hospital, Charlestown, MA, USA

Corresponding Author: Daiki Sasabayashi, M.D., Ph.D.

Psychiatry Neuroimaging Laboratory

Brigham and Women's Hospital, Harvard Medical School

399 Revolution Drive Suite 1155

Somerville, MA 02145

Tel.: 617-992-5485

E-mail: ds179@med.u-toyama.ac.jp

The running title: Central olfactory pathway and odor recognition

Word counts:

Abstract: 199 words

Article body: 4819 words

Numbers of figures, tables, and supplemental material:

Figures: 5

Tables: 4

Supplemental material: 1

Abstract

Olfactory processing constitutes a unique system where sensory input is directly linked to integrative perceptual processing, providing an optimal model for investigating how perceptual input is transformed into higher-order functions. However, the neural substrates of olfaction remain incompletely understood. Here, we delineated central olfactory pathways using advanced tractography and examined associations between tractography metrics and olfactory functions. We acquired T1-weighted and diffusion-weighted images from 129 healthy participants and assessed olfactory function in 59 individuals using a T&T olfactometer. We defined the primary olfactory cortex and secondary olfactory structures and their connections. White matter query language was used to extract central olfactory pathways from refined whole-brain tractography according to neuroanatomical rules. We analyzed the number of streamlines and the laterality index of these pathways in relation to olfactory detection and recognition thresholds. For the total olfactory fascicle, more streamlines were observed in the left than the right hemisphere, and greater leftward lateralization was significantly associated with lower mean recognition thresholds. In conclusion, we successfully reconstructed central olfactory pathways beyond the primary olfactory cortex and provided evidence supporting the neural basis of higher-order olfactory functions. Leftward lateralization may enhance associative olfactory processing by reducing circuit redundancy and allocating additional neural capacity.

Key words: Olfactory pathway; Olfactory function; Tractography; White matter; Diffusion imaging

Introduction

Human olfaction supports critical cognitive and behavioral characteristics, including food intake, social interaction, memory formation, and environmental threat detection (Gottfried 2010). The olfactory system comprises a combination of peripheral sensory processing (mainly in the olfactory epithelium, olfactory bulb, and olfactory tract) and cerebral integrative perceptual processing (centered on the primary olfactory cortices and secondary olfactory structures) (Seubert et al. 2013). Notably, and unlike other sensory systems, olfactory input projects directly to the olfactory cortex without thalamic relay (Carmichael et al. 1994; Zhang et al. 2024). This anatomical distinctiveness implies that sensory stimuli are processed in direct association with higher-order integrative processes, including semantic association, affective evaluation, and memory retrieval (Kadohisa 2013). Accordingly, elucidating the neural substrates of olfaction, particularly the olfactory pathways, may provide a valuable model for understanding how sensory input is transformed into higher-order perceptual functions (Kehl et al. 2024).

Accumulating evidence has begun to demonstrate the relationship between structural features of the olfactory pathway and olfactory function. Olfactory bulb volume has been positively correlated with olfactory performance (Yousem et al. 1998; Buschhuter et al. 2008; Seubert et al. 2013; Mazal et al. 2016). In individuals with olfactory loss, reduced volume of primary olfactory cortex and secondary olfactory structures (Bitter et al. 2010) and decreased fractional anisotropy (FA) in the white matter surrounding the primary olfactory area (Ibarretxe-Bilbao et al. 2010) have been observed. In our previous study, across both healthy individuals and individuals with psychiatric disorders, shallower olfactory sulcus depth was associated with superior

odor identification (Takahashi et al. 2019). Recent tractography investigations have delineated the olfactory tracts, revealing that higher mean diffusivity within these tracts correlates with poorer odor discrimination performance (Echevarria-Cooper et al. 2022). However, studies examining the relationship with olfactory function have been largely confined to localized structures or the peripheral olfactory system.

To date, few tractography studies have attempted to delineate the white matter fascicles underlying the central olfactory pathway, which serves higher-order olfactory functions such as odor recognition (Haberly et al. 2001). One potential reason is the lack of consensus regarding its anatomical organization, in contrast to the well-characterized visual and auditory systems (Zhou et al. 2019). Detailed knowledge of the precise projection patterns to the olfactory cortex and the organization of parallel functional pathways in humans remains limited. Additionally, the olfactory pathway is thin, highly branched, and anatomically complex, making it difficult to reconstruct using conventional tractography techniques (Echevarria-Cooper et al. 2022). Furthermore, substantial interindividual variability in olfactory anatomy poses a challenge, as atlas-based registration fails to account for subject-specific anatomical variability (Fjaeldstad et al. 2017).

The present study aims to delineate the central olfactory pathway by employing precisely defined regions of interest (ROIs) determined by neuroanatomical experts and advanced tractography techniques. Specifically, we applied tractography with sophisticated modeling and the White Matter Query Language (WMQL), an automated tool for segmenting fiber bundles based on any brain atlas (Wasserman et al. 2016). Beyond automation, WMQL enables rule-based extraction of fiber fascicles in each subject's native space. While conventional manual delineation suffers from limited

reproducibility (Zhang et al., 2010), WMQL preserves comparable precision while enabling rapid and consistent tract extraction (Wassermann et al. 2016). Unlike clustering-based methods that rely on geometric features and lack clear anatomical interpretability (O'Donnell and Westin 2007), WMQL is grounded in expert defined neuroanatomical rules, allowing anatomically meaningful delineation of white matter fascicles. The primary objective of this study is to elucidate the neural basis of higher-order olfactory functions by investigating the relationship between tractography metrics and olfactory performance in healthy individuals.

Materials and methods

Participants

A total of 131 healthy control (HC) individuals were initially enrolled at Toyama University Hospital between August 2012 and November 2023. During image preprocessing, two HC participants were excluded, leaving 129 subjects for the final imaging analysis (median age, 25 years; range, 20-40 years). All of these 129 individuals had also taken part in our earlier work (Sasabayashi et al. 2025), which examined associations between white matter microstructure and saturated fatty acids in individuals with clinical high-risk for psychosis as well as in HC. Recruitment targeted hospital employees, university students, and residents from the local community. They were eligible only if they completed the SCID-I Non-patient Edition (First et al. 1997) screening and had no psychiatric disorders in themselves or in first-degree relatives. At the time of MRI acquisition, all participants were in good physical condition, with no record of major head trauma, neurological disorders, corticosteroid treatment, substance misuse, or other severe medical conditions. Cigarette use, handedness (Okada et al.

2014a), and both personal and parental socioeconomic status, determined by educational background (Okada et al. 2014b) were examined. More specifically, socioeconomic status was operationalized using an education-based scale ranging from 1 to 7, with higher scores indicating higher educational attainment. Individual socioeconomic status was based on the participant's highest level of education, while parental socioeconomic status was derived from the highest educational attainment of the parents. In addition, participants completed the Japanese version of the State-Trait Anxiety Inventory (STAI-JYZ) (Iwata et al. 1998) to provide self-reported measures of their state and trait anxiety during the olfactory evaluation. All 129 participants had diffusion-weighted imaging data and were included in the tractography analyses, while a subset of 59 participants additionally underwent olfactory function assessment (detailed below). All volunteers gave written informed consent after being fully informed of the study procedures and goals, in line with the Declaration of Helsinki. Ethical approval for this project was granted by the Committee of Medical Ethics of the University of Toyama (No. R2013131).

Image acquisition

Study participants underwent MRI scanning on a 3.0 T Siemens Magnetom Verio system (Siemens Medical Systems, Erlangen, Germany) equipped with a 12-channel head coil. Diffusion-weighted data were acquired using two-dimensional echo-planar imaging (EPI) (TR = 11.5 s, TE = 87 ms [89 ms for 11 participants due to a temporary software update issue], matrix = 112 × 112, field of view = 224 × 224 mm, voxel size = 2 × 2 × 2 mm, 75 slices, 30 non-collinear directions, b = 0 and 1000 s/mm^2). Structural T1-weighted images were obtained with a three-dimensional magnetization prepared

rapid gradient echo sequence (MPRAGE) sequence (TR = 2300 ms, TE = 2.9 ms, flip angle = 9°, matrix = 256 × 256, field of view = 256 mm, voxel size = 1.0 × 1.0 × 1.2 mm, 176 slices).

Image preprocessing

Imaging data were analyzed using our in-house pipeline (https://github.com/pnlbwh/luigi-pnlpipe) that combines various processing modules. Diffusion-weighted images from 131 subjects were transformed from DICOM into NIfTI format, realigned, re-centered, and then inspected using a semi-automated quality control procedure. Two participants were excluded due to significant signal dropouts after visual inspection using 3D slicer (v.4.10; www.slicer.org). Subsequently, Gibbs ringing artifact removal was applied (Kellner et al. 2016). Brain extraction, involving the removal of non-brain tissue from the skull region, was performed using a convolutional neural network-based method (Guha et al. 2019). Motion related artifacts and eddy current distortions were subsequently corrected with the Functional Magnetic Resonance Imaging of the Brain Software Library (FSL) (Smith et al. 2004). Furthermore, distortions arising from EPI were adjusted to reduce signal attenuation and voxel displacement associated with magnetic field irregularities and interactions (Andersson et al. 2003).

For structural imaging, DICOM files of T1-weighted scans were obtained from 131 participants, converted to NIfTI format, and subsequently aligned to standard axes and centered. Brain masks for T1-weighted images were generated using the high-definition brain extraction tool (HD-BET) (Isensee et al. 2019), followed by visual quality inspection and manual editing when necessary. The brain gray matter was

parcellated into 68 regions according to the Desikan-Killiany atlas (Desikan et al. 2006) using FreeSurfer (v7.1.0) (Fischl 2012). In addition, the Human Connectome Project Multi-Modal Parcellation version 1.0 (HCP-MMP1) atlas (Glasser et al. 2016) was mapped onto individual T1 weighted images using registration-based approaches. Intracranial volume was estimated at this time.

Whole-brain tractography

Whole-brain tractography data was generated from the preprocessed diffusion data with a b-value of 1000 s/mm² using the Unscented Kalman Filter (UKF) tractography approach. UKF improves the precision of fiber reconstruction by integrating information from previous tracking steps (Malcolm et al. 2010; Reddy et al. 2016). Whole-brain white matter fiber bundles were reconstructed using a two-tensor model to detect intersecting fibers (Farquharson et al. 2013; Vos et al. 2013) alongside free-water modelling to maintain accurate fiber orientation by minimizing interference from extracellular free-water (Liao et al. 2017). Streamlines were propagated from voxels within the brain mask with FA above 0.06 and using ten seeds per voxel. Streamline propagation was terminated when FA fell below 0.05 or the normalized mean signal fell below 0.05. These relatively permissive thresholds were selected to enhance the sensitivity of tract reconstruction for the olfactory pathway. To prevent bias from excessively short fibers, only trajectories longer than 40 mm were retained (Guevara et al. 2012; Jin et al. 2014; Lefranc et al. 2016).

Anatomical definition of olfactory cortex

The olfactory pathway exhibits inconsistencies in its definition (Soudry et al. 2011; Misiak et al. 2017; Han et al. 2019) and inter-individual variation (Covantev et al. 2019; Zhou et al. 2019). Therefore, we defined the olfactory pathway of interest in consultation with neuroanatomical experts N.M. and R.J.R. Whereas the spatial resolution of diffusion imaging limits visualization of the fine olfactory nerve axons extending from the olfactory nerves through the bulb to the cortex, nerve axon fascicles beyond the olfactory cortex can be reliably delineated (Kurihara et al. 2022). We thus depicted the central olfactory pathways, focusing on projections from the primary olfactory cortex to the secondary olfactory structures, using advanced diffusion imaging techniques (i.e., whole-brain tractography with hybrid modeling followed by reproducible white matter pathway extraction using defined regions of interest) (Figure 1). This focus is justified as post-primary olfactory projections are especially informative for elucidating higher-order olfactory functions, including odor recognition (Haberly et al. 2001).

We defined the olfactory brain structures as follows (Figure 2). Piriform cortex was designated as the primary olfactory cortex because it receives the largest input from the olfactory bulb and is extensively interconnected with higher order olfactory cortices (Price 1990). Based on prior studies (Price 1991; Carmichael et al. 1994; Mehedano-Moriano et al. 2007; Freese and Amaral 2009), the principal projection targets of the primary olfactory cortex were designated as secondary olfactory structures, including the amygdala, hippocampus, thalamus, insula, and orbitofrontal cortex (OFC). The secondary olfactory structures were further restricted to subfields specifically implicated in olfactory processing (Price 1991; Carmichael et al. 1994; Markis et al. 1999; Poellinger et al. 2001; Noto et al. 2021; Haehner et al. 2022; Menelaou et al. 2022).

Piriform cortex: Piriform cortex label derived from the HCP-MMP1 atlas (Glasser et al. 2016), consistent with the atlas of Mai et al. (2016)

Amygdala (anterior and medial parts): Combined labels of medial, cortical, cortico-amygdaloid transition area, and anterior amygdala area derived from the FreeSurfer amygdala subfields atlas (Saygin et al. 2017)

Hippocampus (relevant parts): Combined labels of CA1, CA3, CA4, Granule cell and molecular layers of the dentate gyrus (GC-ML-DG), molecular layer, subiculum, and hippocampal tail derived from the FreeSurfer hippocampal subfields atlas (Iglesias et al. 2015)

Thalamus (medial and dorsal parts): Combined labels of mediodorsal medial magnocellular, mediodorsal lateral parvocellular, and centromedian derived from the FreeSurfer thalamic subfields atlas (Iglesias et al. 2018)

Insula (rostral part): Combined labels of anterior agranular insula complex, anterior ventral insular area, middle insular area, and insular granular complex derived from the HCP-MMP1 atlas (Glasser et al. 2016)

OFC (caudal part): Combined labels of posterior OFC complex and orbital frontal complex derived from the HCP-MMP1 atlas (Glasser et al. 2016)

Based on prior literature (Price 1991; Carmichael et al. 1994; Nieuwenhuys et al. 2008), we also defined exclusion brain regions through which the olfactory pathway has not been identified to pass, to allow precise extraction of white matter fascicles. All regions are defined using labels derived from the Desikan-Killiany atlas (Desikan et al. 2006).

Medial parietal cortex: superior parietal, inferior parietal, supramarginal, postcentral, precuneus, and paracentral

Frontal motor cortex: precentral, caudal middle frontal, rostral middle frontal, superior frontal, and frontal pole

Occipital cortex: lateral occipital, lingual, cuneus, and pericalcarine

visuotemporal cortex: fusiform, inferior temporal, middle temporal, superior temporal, and banks of the superior temporal sulcus (bankssts)

Auditory cortex: transverse temporal, superior temporal, and bankssts

Cingulate cortex: rostral anterior cingulate, caudal anterior cingulate, posterior cingulate, and isthmus cingulate

Finally, these parcellations were registered from T1-weighted to diffusion-weighted imaging space through rigid registration using the Advanced Normalization Tools (ANTs) software. The resulting parcellations retained correspondence with standardized anatomical coordinates in Montreal Neurological Institute (MNI) space, enabling the definition of endpoints and waypoints for tractography.

Extraction of olfactory pathway

White Matter Query Language (WMQL) was applied as an automated framework to extract specific white matter fascicles from whole-brain tractography, relying on anatomically defined brain regions provided by any chosen atlas (Wassermann et al. 2016). Within WMQL, each fascicle is defined through the use of assignment operations. The function “endpoints_in” identifies streamlines whose initial or terminal

point lies within a specified region, thereby delineating connections that originate or terminate in that region. The logical operator “and” designates streamlines that traverse all specified regions, whereas “or” selects streamlines that pass through at least one of them. The operator “not in” excludes streamlines that traverse the specified region, thereby enabling subtraction of sets from the fascicle definition. In this study, we extracted the olfactory fascicle using the olfactory cortex described above and the following assignment expressions (Figure 3). Because the majority of central olfactory fiber fascicles project ipsilaterally (Savic and Gulyas 2000; Collins et al. 2018), we delineated the olfactory pathways of the left and right hemispheres separately, with the equation also specifying exclusion from the opposite hemisphere. The bilateral number of streamlines was calculated as the sum across both hemispheres.

Left total olfactory fascicle = endpoints_in(left piriform cortex) and (left amygdala or left hippocampus or left thalamus or left insula or left OFC) not in right hemisphere not in left medial parietal cortex not in left frontal motor cortex not in left occipital cortex not in left visuotemporal cortex not in left auditory cortex not in left cingulate cortex
Right total olfactory fascicle = endpoints_in(right piriform cortex) and (right amygdala or right hippocampus or right thalamus or right insula or right OFC) not in left hemisphere not in right medial parietal cortex not in right frontal motor cortex not in right occipital cortex not in right visuotemporal cortex not in right auditory cortex not in right cingulate cortex

For supplementary analyses, we also extracted more subdivided white matter fascicles of the olfactory pathway that pass exclusively through each secondary

olfactory structure: olfactory amygdala fascicle, olfactory hippocampus fascicle, olfactory thalamus fascicle, olfactory insula fascicle, olfactory OFC fascicle. Each assignment expression is described in Supplementary Methods 1.

We measured the number of streamlines as the primary tractography metric, as it reflects the relative strength of white matter connectivity and may influence synaptic transmission and subsequent functional interactions across brain regions (Huang and Ding 2016). Given the critical role of hemispheric lateralization in sensory pathways (Cavelius et al. 2022), lateralization indices (LI) of streamline counts were also assessed.

Olfactory function

Detailed information regarding the olfactory testing procedures is described in our previous paper (Takahashi et al. 2015). Briefly, odor detection and recognition were assessed using a T&T olfactometer (Daiichi Yakuhin Sangyo, Tokyo, Japan) with five odorants: odor A (rose), odor B (caramel), odor C (rotten food), odor D (sweet fruit), and odor E (fecal material). Tests lasted 15 to 30 minutes and were conducted by either a clinical laboratory technician (H.I.) or a trained psychiatrist (T.T.) in a ventilated room maintained at 20 to 25°C, with air purified by a cleaner (SD-1; Nagashima medical instruments, Tokyo, Japan). Participants refrained from eating for at least one hour prior to the test, and smokers did not smoke for 30 minutes before testing. Each odorant, dissolved in propylene glycol, was presented at eight increasing concentrations from -2 (lowest) to +5 (highest) using litmus paper strips. The detection threshold was defined as the concentration at which an odor was first noticed, while recognition threshold corresponded to the concentration where the odor was correctly identified. Lower

threshold values indicated better olfactory function. Individual scores were averaged across the five odorants, and a mean recognition threshold of 1.0 or lower indicated normal olfaction.

Statistical analysis

We used the number of streamlines and their LI as tractography-derived measures of the olfactory pathways. LI is calculated using the following formula:

$$LI = \frac{Left - Right}{Left + Right}$$

A positive LI indicates left lateralization, whereas a negative LI indicates right lateralization. We employed SPSS version 27.0.1.0 (IBM Corp., Armonk, NY) for the following statistical analyses.

A one-way analysis of variance (ANOVA) for continuous variables and the chi-square test for categorical variables were used to compare group differences in demographic characteristics and brain volume (i.e., intracranial volume and bilateral piriform cortex volume) between males and females. The non-parametric Mann-Whitney U-test was used to evaluate olfactory abilities (detection and recognition thresholds for mean and each of the five odorants), which were not normally distributed as determined by the Kolmogorov-Smirnov test. The statistical significance threshold was set at $p < 0.05$. For each olfactory rating, Bonferroni-corrected thresholds were applied ($p < 0.05/6$ ratings = 0.0083, two-tailed).

The paired t-test was used to compare the number of streamlines in the total olfactory fascicle between the left and right hemisphere ($p < 0.05$, two-tailed). If significant, analogous t-tests were conducted for the subdivided olfactory fascicles ($p <$

0.05/5 fascicles = 0.01, two-tailed).

Although a recent study reported larger olfactory bulb volumes in males than in females (Hsieh et al., 2026), sex differences in the structural connectivity of the olfactory pathway remain poorly understood. We therefore conducted exploratory analyses to examine potential sex differences in olfactory fascicle streamline counts and their lateralization. ANOVA was additionally used to compare the number of streamlines in the total olfactory fascicle between males and females, controlling for intracranial volume. If significant, analogous ANOVA was performed for the subdivided olfactory fascicles ($p < 0.05/5$ fascicles = 0.01, two-tailed). The LI of the number of streamlines in the total olfactory fascicle between males and females was also compared using ANOVA.

Given the skewed distributions of these variables, Spearman's rank correlation tests were used to examine the relationships between the number of streamlines in the total olfactory fascicle or their LI and representative olfactory ratings (i.e., mean detection or recognition threshold). Prior to correlation analyses, streamline numbers were adjusted for the effect of total piriform cortex volumes (sum of both hemispheres). This was done to account for inter-individual variability in piriform size, as all streamlines were constrained to pass through the piriform cortex. The statistical threshold was set at $p < 0.05/ 2$ variables × 2 ratings = 0.0125, applying Bonferroni correction for multiple comparisons corrections. If significant, supplementary analyses included analogous Spearman's rank correlation analyses for each subdivided olfactory fascicles ($p < 0.05/5$ fascicles = 0.01) or each odor threshold ($p < 0.05/5$ odors = 0.01). To account for potential confounding effects of anxiety symptoms on olfactory function (Takahashi et al. 2015), we conducted supplementary analyses of the associations

between olfactory fascicle streamlines and olfactory ratings with additional adjustment for anxiety scores (i.e., STAI trait and STAI state). Considering that handedness may influence hemispheric structural asymmetry (Sha et al. 2021), we also performed supplementary analyses controlling for handedness.

Results

Characteristics of study participants

The characteristics of the participants by sex are summarized in Table 1. Compared with males, females were younger and had lower socioeconomic status and parental socioeconomic status. Females had smaller intracranial and bilateral piriform volumes than males. Females exhibited a tendency toward higher detection thresholds for odor C, elevated recognition thresholds for odor C, and reduced recognition thresholds for odor E relative to males; however, none of these differences retained statistical significance following Bonferroni correction. There were no sex differences in the prevalence of subclinical olfactory deficits.

Number of Olfactory fascicle streamlines and their laterality

The total olfactory fascicle was detected in all participants. The olfactory amygdala fascicle, olfactory insula fascicle, and olfactory OFC fascicle were also present in all 129 participants (100%). However, the olfactory hippocampus fascicle was present in 125 participants (96.9%) and the olfactory thalamus fascicle was identified in 104 participants (80.6%).

The left total olfactory fascicle exhibited a significantly greater number of streamlines than the right total olfactory fascicle (Table 2). Post-hoc analyses revealed

that the left olfactory OFC fascicle also included significantly more streamlines than the right olfactory OFC fascicle, whereas the right olfactory amygdala fascicle contained significantly more streamlines than the left olfactory amygdala fascicle (Table 2). The LI of the total olfactory fascicle was positive, indicating left lateralization, likely driven by the LI of the olfactory OFC fascicle (Table 3).

Group comparisons of olfactory fascicle streamlines between males and females

Males exhibited a significantly greater number of streamlines in the total olfactory fascicle compared with females (Table 4). Given the demographic differences between males and females, we controlled for age, personal and parental socioeconomic status as well as intracranial volume. The intergroup difference in the number of streamlines remained significant ($F[1,128] = 5.613$, $p = 0.019$). In post-hoc analyses, males had significantly more streamlines than females only in the olfactory OFC fascicle (Table 4). The LI of the total olfactory fascicle did not differ between males (Mean = 0.174, SD = 0.328) and females (Mean = 0.106, SD = 0.346) ($F[1,128] = 1.345$, $p = 0.248$).

Relationships between olfactory fascicle streamlines and olfactory ratings

A higher LI of the total olfactory fascicle (i.e., greater left lateralization) was significantly associated with lower mean recognition thresholds (i.e., enhanced identification ability) (Figure 4; Figure 5A). At the tract-specific level, a similar negative correlation with mean recognition thresholds was observed exclusively for the LI of the olfactory insula fascicle (Supplementary Table 1; Figure 5B). At the odor-specific level, a comparable negative correlation with the LI of the total olfactory fascicle was found only for odor E (Supplementary Table 2; Figure 5C). In the

supplementary analyses, the significant negative correlation between the LI of the total olfactory fascicle and mean recognition thresholds was preserved even after controlling for STAI trait (r = -0.369, p = 0.004) and STAI state (r = -0.375, p = 0.003). Additionally, this association remained significant when handedness was included as a covariate (r = -0.381, p = 0.003). The number of streamlines in the total olfactory fascicle was not significantly associated with mean detection or recognition threshold (Figure 4).

Discussion

We present, for the first time in diffusion imaging, a delineation of white matter fascicles representing the central olfactory pathway and an examination of their relationship with olfactory function. In healthy participants, the number of streamlines representing the total olfactory fascicle was greater in the left hemisphere than in the right hemisphere, likely driven by a higher number of streamlines in the olfactory OFC fascicle. The LI of the total olfactory fascicle also indicated leftward lateralization of streamline counts. Males exhibited significantly more streamlines than females in the total olfactory fascicle, particularly within the olfactory OFC fascicle. A higher LI of the total olfactory fascicle was significantly associated with lower mean recognition thresholds, with this association most evident for the LI of the olfactory insula fascicle and recognition thresholds for odor E.

As the olfactory pathway is anatomically predominantly ipsilateral, it allows a relatively precise assessment of structural lateralization with fewer confounding factors compared with other sensory systems (Cavelius et al. 2022). The present study demonstrated leftward lateralization of the anatomical architecture of the olfactory

pathway in healthy individuals, in terms of the number of tractography-derived streamlines. Recent research similarly reported left hemisphere predominance, with 73% of intrahemispheric structural connectivity fibers from the primary olfactory cortex to secondary olfactory structures located in the left hemisphere (Fjaeldstad et al. 2021). Interestingly, during odor mental imagery, non-expert participants exhibited left-lateralized event-related potential amplitudes, whereas cooking experts showed bilateral symmetry, suggesting that professional expertise may modulate the lateralization of olfactory neural substrates (Bensafi et al. 2017). Therefore, future investigations are warranted to elucidate whether this lateralization of the olfactory pathway reflects an innate trait or is influenced by learning and experience.

Our principal finding was that the LI of streamlines passing beyond the primary olfactory cortex was associated with recognition thresholds rather than detection thresholds, particularly for the olfactory insula fascicle and odor E recognition. This aligns with the notion that categorical odor representations depend on piriform associative connections (Barnes and Wilson 2014; Bao et al. 2016). Odor discrimination learning in animals induced dynamic leftward bias in the piriform cortex (Cohen et al. 2015). Such lateralization may enhance associative olfactory processing through inter-hemispheric functional separation, allowing simultaneous and specialized processing of distinct olfactory dimensions rather than redundant bilateral processing of similar information (Cohen and Wilson 2017). Consequently, individuals with more pronounced left lateralization of central olfactory pathways may possess more efficient neural circuits for odor identification. Among the secondary olfactory structures receiving piriform projections, hemispheric asymmetry in the insula has been linked to olfactory cognition performance. Olfactory quality discrimination significantly

correlates with insular cortical thickness (Frasnelli et al. 2010), and lateralized insular activity has been observed during odor memory tasks (Dade et al. 2002). Conversely, prior studies on odor type and functional connectivity remain inconclusive: some report a correlation between odor pleasantness and neural activity in the left OFC (Rolls et al. 2003), whereas others report that unpleasant odors preferentially activate the left OFC (Gottfried et al. 2002). However, our study did not evaluate subjective pleasantness or unpleasantness of odors. Interestingly, aversive stimulus coding has been observed in the anterior insula in some other sensory systems (Simmons et al. 2004; Caria et al. 2010; Linnman et al. 2013). Furthermore, structural and functional connectivity do not necessarily share identical functional implications (Honey et al. 2009). Future multimodal studies combining functional MRI and diffusion imaging are warranted to provide an integrated assessment of the relationship between brain connectivity and olfactory function, including subjective odor assessments.

Females tend to outperform males in both odor detection and recognition (Doty and Cameron 2009), although the neural correlates supporting this have yet to be detected (Bengtsson et al. 2001). In light of this evidence, our finding that females exhibited fewer olfactory fascicle streamlines than males, even after adjusting for intracranial volume, was unexpected. However, streamline counts were not associated with any olfactory ratings. Furthermore, the absence of sex differences in the LI of olfactory fascicle streamlines is consistent with the lack of observed sex differences in olfactory function within this sample. One possible explanation is that the present subsample, in which both olfactory function and diffusion imaging were assessed, was underpowered, given that our previous study with a larger sample reported superior olfactory performance in females (Takahashi et al. 2015). Another possibility is that the

sex difference in streamline counts may reflect non-olfactory functions, given prior links between limbic pathways (e.g., amygdala and OFC) and emotional regulation and reward valuation (Bracht et al. 2014).

Several limitations should be acknowledged. First, the tractography in this study was based on single-shell diffusion data. Compared with multi-shell diffusion data, single-shell acquisitions are more susceptible to noise and artifacts, increasing the likelihood of false positives or omissions during deterministic tract reconstruction (Jbabdi et al. 2013). Due to the limited imaging quality, the tendency for diffusion signals to drop or attenuate in fronto-orbital and temporal regions may have an impact on results, despite the artifact correction procedures, and deserve further consideration (Lahti et al. 2021). Second, the streamline metrics employed here did not include pathways preceding the primary olfactory cortex such as the olfactory bulb, whereas ideally, the entire pathway from the olfactory epithelium and bulb should be reconstructed. Inclusion of these peripheral segments as part of the reconstructed olfactory tract could introduce additional variance related to a short-term habituation process mediated at the epithelial and bulbar levels (Ogg et al. 2015). This additional variance could potentially obscure or confound the observed associations between central olfactory pathway metrics and olfactory cognitive function. Finally, olfactory function is closely linked to emotional processing, sharing common neural substrates (Soudry et al. 2011), and confounding effects of differential emotional status across individuals warrant further investigation. In our supplementary analyses, the significant associations between the LI of streamlines and olfactory performance remained even after adjusting for anxiety symptoms. Nevertheless, disentangling potential confounding effects arising from inter-individual differences in context-dependent emotional

regulation (Kadohisa et al. 2013) remains a challenge for future research.

In conclusion, through the application of advanced tractography techniques, we successfully delineated the olfactory pathway beyond the primary olfactory cortex and provided preliminary evidence regarding the neural substrates of high-order olfactory function. In healthy individuals, olfactory fascicles were generally left-lateralized, with greater leftward lateralization associated with superior olfactory recognition performance. Although males exhibited a greater number of olfactory fascicles than females, the functional significance remains to be clarified. Future innovations in neuroimaging techniques are expected to enable reconstruction of the entire olfactory pathway beginning at the olfactory epithelium.

Acknowledgements

The authors extend their gratitude to all participants for their invaluable contributions to this study, as well as to the research staff responsible for data collection and management.

Funding

The present study was supported by JSPS KAKENHI Grant Numbers JP18K15509 and JP22K15745 to D.S., JP16K10205 and JP22K07554 to Y.Higuchi., JP24K02378 to S.K., JP20KK0193, JP21H02851, and JP23K21414 to Y.Hirano., JP24K10704 to T.T., AMED Grant Numbers JP256f0137012 to D.S., and H.T., JP24wm0625302 to T.T., Y.Hirano., and S.K. The current study was also supported by NIMH Grant Numbers U01MH109977 to M.E.S., U24MH124629-01 to M.E.S., R01MH102377 to M.K., M.E.S., R01MH136503 to M.K., R01MH119222 to Y.R., R01MH112748 to M.K., N.M., R01MH125860 to N.M., Y.R., R01NS125307 to R.J.R., N.M., Y.R., K24MH116366 to N.M. H.I would like to acknowledge the training received under the Scholars in Health Research Program (SHARP) that was in part supported by the Fogarty International Center and Office of Dietary Supplements of the National Institutes of Health (Award Number D43 TW009118). We also acknowledge funding provided by the Brain and Behavior Research Foundation (BBRF): NARSAD Distinguished Investigator Award to M.K.

Data Availability

The datasets generated and analyzed during the current study are not publicly available due to reasons of data privacy and regulatory/ethical approvals, but aggregate-level data

are available from the corresponding author upon reasonable request and pending local and national data protection and ethics regulations.

Conflict of Interest

The authors declare no competing interests.

Author Contributions

In this study, D.S., T.T., M.K., and R.J.R. conceived the conception and design of this study. D.S., H.Itoh., H.T., Y.Higuchi., K.N., and T.T. contributed to data acquisition. D.S., Y.R., J.H.R., K.K., H.Iaali., N.M., M.K., and R.J.R. analyzed the data. S.K., Y.Hirano., and M.E.S. provided advice on data analysis. D.S., M.K., and R.J.R. drafted the manuscript. All authors contributed to revise the manuscript and have approved the final manuscript.

References

Andersson JL, Skare S, Ashburner J (2003) How to correct susceptibility distortions in spin-echo echo-planar images: application to diffusion tensor imaging. Neuroimage. 20(2):870-88. https://doi.org/10.1016/S1053-8119(03)00336-7

Bao X, Raguet LL, Cole SM, Howard JD, Gottfried J (2016) The role of piriform associative connections in odor categorization. Elife. 5:e13732. https://doi.org/10.7554/eLife.13732

Barnes DC, Wilson DA (2014) Slow-wave sleep-imposed replay modulates both strength and precision of memory. J Neurosci. 34(15):5134-5142. https://doi.org/10.1523/JNEUROSCI.5274-13.2014

Bengtsson S, Berglund H, Gulyas B, Cohen E, Savic I (2001) Brain activation during odor perception in males and females. Neuroreport. 12(9):2027-2033. https://doi.org/10.1097/00001756-200107030-00048

Bensafi M, Fournel A, Joussain P, Poncelet J, Przybylski L, et al (2017) Expertise shapes domain-specific functional cerebral asymmetry during mental imagery: the case of culinary arts and music. Eur J Neurosci. 45(12):1524-1537. https://doi.org/10.1111/ejn.13596

Bitter T, Brüderle J, Gudziol H, Burmeister HP, Gaser C, et al (2010) Gray and white matter reduction in hyposmic subjects--A voxel-based morphometry study. Brain Res. 1347:42-47. https://doi.org/10.1016/j.brainres.2010.06.003

Bracht T, Horn H, Strik W, Federspiel A, Razavi N, et al (2014) White matter pathway organization of the reward system is related to positive and negative symptoms in schizophrenia. Schizophr Res. 153(1-3):136-142. https://doi.org/10.1016/j.schres.2014.01.015

Buschhüter D, Smitka M, Puschmann S, Gerber JC, Witt M, et al (2008) Correlation between olfactory bulb volume and olfactory function. Neuroimage. 42(2):498-502. https://doi.org/10.1016/j.neuroimage.2008.05.004

Caria A, Sitaram R, Veit R, Begliomini C, Birbaumer N (2010) Volitional control of anterior insula activity modulates the response to aversive stimuli. A real-time functional magnetic resonance imaging study. Biol Psychiatry. 68:425-434. https://doi.org/10.1016/j.biopsych.2010.04.020

Carmichael ST, Clugnet MC, Price JL (1994) Central olfactory connections in the macaque monkey. J Comp Neurol. 346(3):403-434. https://doi.org/10.1002/cne.903460306

Cavelius M, Brunel T, Didier A (2022) Lessons from behavioral lateralization in olfaction. Brain Struct Funct. 227(2):685-696. https://doi.org/10.1007/s00429-021-02390-w

Cohen Y, Putrino D, Wilson DA (2015) Dynamic cortical lateralization during olfactory discrimination learning. J Physiol. 593(7):1701-1714. https://doi.org/10.1113/jphysiol.2014.288381

Cohen Y, Wilson DA (2017) Task-Correlated Cortical Asymmetry and Intra- and Inter-Hemispheric Separation. Sci Rep. 7(1):14602. https://doi.org/10.1038/s41598-017-15109-x

Collins LN, Hill DL, Brunjes PC (2018) Myelination of the developing lateral olfactory tract and anterior commissure. J Comp Neurol. 526(11):1843-1858. https://doi.org/10.1002/cne.24452

Covanțev S (2018) Cranial nerve I: clinical anatomy and beyond. Russian Open Medical Journal. 7(1):e0101. https://doi.org/10.15275/rusomj.2018.0101

Dade LA, Zatorre RJ, Jones-Gotman M (2002) Olfactory learning: convergent findings from

lesion and brain imaging studies in humans. Brain. 125:86-101. https://doi.org/10.1093/brain/awf003
Desikan RS, Ségonne F, Fischl B, Quinn BT, Dickerson BC, et al (2006) An automated labeling system for subdividing the human cerebral cortex on MRI scans into gyral based regions of interest. Neuroimage. 31(3):968-980. https://doi.org/10.1016/j.neuroimage.2006.01.021
Doty RL, Cameron EL (2009) Sex differences and reproductive hormone influences on human odor perception. Physiol Behav. 97(2):213-228. https://doi.org/10.1016/j.physbeh.2009.02.032
Echevarria-Cooper SL, Zhou G, Zelano C, Pestilli F, Parrish TB, et al (2022) Mapping the Microstructure and Striae of the Human Olfactory Tract with Diffusion MRI. J Neurosci. 42(1):58-68. https://doi.org/10.1523/JNEUROSCI.1552-21.2021
Farquharson S, Tournier JD, Calamante F, Fabinyi G, Schneider-Kolsky M, et al (2013) White matter fiber tractography: why we need to move beyond DTI. J Neurosurg. 118(6):1367-77. https://doi.org/10.3171/2013.2.JNS121294
First MB, Williams JBW, Karg RS, Spitzer RL (2015) Structured clinical interview for DSM-5-Research version (SCID-5 for DSM-5, research version; SCID-5-RV). American Psychiatric Publishing, Washington DC.
Fischl B (2012) FreeSurfer. Neuroimage. 62(2):774-781. https://doi.org/10.1016/j.neuroimage.2012.01.021
Fjaeldstad A, Fernandes HM, Van Hartevelt TJ, Gleesborg C, Møller A, et al (2017) Brain fingerprints of olfaction: a novel structural method for assessing olfactory cortical networks in health and disease. Sci Rep. 7:42534. https://doi.org/10.1038/srep42534
Fjaeldstad AW, Stiller-Stut F, Gleesborg C, Kringelbach ML, Hummel T, et al (2021) Validation of Olfactory Network Based on Brain Structural Connectivity and Its Association With Olfactory Test Scores. Front Syst Neurosci. 15:638053. https://doi.org/10.3389/fnsys.2021.638053
Frasnelli J, Lundström JN, Boyle JA, Djordjevic J, Zatorre RJ, et al (2010) Neuroanatomical correlates of olfactory performance. Exp Brain Res. 201(1):1-11. https://doi.org/10.1007/s00221-009-1999-7
Freese JL and Amaral DG (2009) Neuroanatomy of the primate amygdala. In The human amygdala (eds Whalen PJ and Phelps EA). The Guilford Press, New York, pp 3-42.
Glasser MF, Coalson TS, Robinson EC, Hacker CD, Harwell J, et al (2016) A multi-modal parcellation of human cerebral cortex. Nature. 536(7615):171-178. https://doi.org/10.1038/nature18933
Gottfried JA (2010) Central mechanisms of odour object perception. Nat Rev Neurosci. 11(9):628-641. https://doi.org/10.1038/nrn2883
Gottfried JA, Deichmann R, Winston JS, Dolan RJ (2002) Functional heterogeneity in human olfactory cortex: an event-related functional magnetic resonance imaging study. J Neurosci. 22(24):10819-10828. https://doi.org/10.1523/JNEUROSCI.22-24-10819.2002
Guevara P, Duclap D, Poupon C, Marrakchi-Kacem L, Fillard P, et al (2012) Automatic fiber bundle segmentation in massive tractography datasets using a multi-subject bundle atlas. Neuroimage. 61(4):1083-1099. https://doi.org/10.1016/j.neuroimage.2012.02.071
Guha Roy A, Conjeti S, Navab N, Wachinger C (2019) QuickNAT: A fully convolutional network for quick and accurate segmentation of neuroanatomy. Neuroimage. 186:713-727. https://doi.org/10.1016/j.neuroimage.2018.11.042
Haberly LB (2001) Parallel-distributed processing in olfactory cortex: new insights from

morphological and physiological analysis of neuronal circuitry. Chem Senses. 26(5):551-576. https://doi.org/10.1093/chemse/26.5.551
Haehner A, Chen B, Espin M, Haussmann R, Matthes C, et al (2022) Training with Odors Impacts Hippocampal Thickness in Patients with Mild Cognitive Impairment. J Alzheimers Dis. 88(2):743-755. https://doi.org/10.3233/JAD-220248
Han P, Zang Y, Akshita J, Hummel T (2019) Magnetic Resonance Imaging of Human Olfactory Dysfunction. Brain Topogr. 32(6):987-997. https://doi.org/10.1007/s10548-019-00729-5
Honey CJ, Sporns O, Cammoun L, Gigandet X, Thiran JP, et al (2009) Predicting human resting-state functional connectivity from structural connectivity. Proc Natl Acad Sci U S A. 106(6):2035-2040. https://doi.org/10.1073/pnas.0811168106
Hsieh YT, Liao YC, Dulnuan HGP, Lirng JF, Chao YT (2026) Sex differences modulate olfactory bulb volume-function relationships but not olfactory training-induced plasticity. Brain Struct Funct. 231(5):73. https://doi.org/10.1007/s00429-026-03126-4
Huang H, Ding M (2016) Linking Functional Connectivity and Structural Connectivity Quantitatively: A Comparison of Methods. Brain Connect. 6(2):99-108. https://doi.org/10.1089/brain.2015.0382
Ibarretxe-Bilbao N, Junque C, Marti MJ, Valldeoriola F, Vendrell P, et al (2010) Olfactory impairment in Parkinson's disease and white matter abnormalities in central olfactory areas: A voxel-based diffusion tensor imaging study. Mov Disord. 25(12):1888-1894. https://doi.org/10.1002/mds.23208
Iglesias JE, Insausti R, Lerma-Usabiaga G, Bocchetta M, Van Leemput K, et al (2015) A computational atlas of the hippocampal formation using ex vivo, ultra-high resolution MRI: Application to adaptive segmentation of in vivo MRI. Neuroimage. 115:117-137. https://doi.org/10.1016/j.neuroimage.2015.04.042
Iglesias JE, Insausti R, Lerma-Usabiaga G, Bocchetta M, Van Leemput K, et al (2018) A probabilistic atlas of the human thalamic nuclei combining ex vivo MRI and histology. Neuroimage. 183:314-326. https://doi.org/10.1016/j.neuroimage.2018.08.012
Isensee F, Schell M, Pflueger I, Brugnara G, Bonekamp D, et al (2019) Automated brain extraction of multisequence MRI using artificial neural networks. Hum Brain Mapp. 40(17):4952-4964. https://doi.org/10.1002/hbm.24750
Iwata N, Mishima N, Shimizu T, Mizoue T, Fukuhara M, et al (1998) Positive and negative affect in the factor structure of the State-Trait Anxiety Inventory for Japanese workers. Psychol Rep. 82(2):651-656. https://doi.org/10.2466/pr0.1998.82.2.651
Jbabdi S, Sotiropoulos SN, Savio AM, Graña M, Behrens TE (2012) Model-based analysis of multishell diffusion MR data for tractography: how to get over fitting problems. Magn Reson Med. 68(6):1846-1855. https://doi.org/10.1002/mrm.24204
Jin Y, Shi Y, Zhan L, Gutman BA, de Zubicaray GI, et al (2014) Automatic clustering of white matter fibers in brain diffusion MRI with an application to genetics. Neuroimage. 100:75-90. https://doi.org/10.1016/j.neuroimage.2014.04.048
Kadohisa M (2013) Effects of odor on emotion, with implications. Front Syst Neurosci. 7:66. https://doi.org/10.3389/fnsys.2013.00066
Kehl MS, Mackay S, Ohla K, Schneider M, Borger V, et al (2024) Single-neuron representations of odours in the human brain. Nature. 634(8034):626-634. https://doi.org/10.1038/s41586-024-08016-5
Kellner E, Dhital B, Kiselev VG, Reisert M (2016) Gibbs-ringing artifact removal based on local subvoxel-shifts. Magn Reson Med. 76(5):1574-1581.

https://doi.org/10.1002/mrm.26054
Kurihara S, Tei M, Hata J, Mori E, Fujioka M, et al (2022) MRI tractography reveals the human olfactory nerve map connecting the olfactory epithelium and olfactory bulb. Commun Biol. 5(1):843. https://doi.org/10.1038/s42003-022-03794-y
Lahti K, Parkkola R, Jaasaari P, Haataja L, Saunavaara V (2021) The impact of susceptibility correction on diffusion metrics in adolescents. Pediatr Radiol. 51(8):1471-1480. https://doi.org/10.1007/s00247-021-05000-3
Lefranc S, Roca P, Perrot M, Poupon C, Le Bihan D, et al (2016) Groupwise connectivity-based parcellation of the whole human cortical surface using watershed-driven dimension reduction. Med Image Anal. 30:11-29. https://doi.org/10.1016/j.media.2016.01.003
Liao R, Ning L, Chen Z, Rigolo L, Gong S, et al (2017) Performance of unscented Kalman filter tractography in edema: Analysis of the two-tensor model. Neuroimage Clin. 15:819-831. https://doi.org/10.1016/j.nicl.2017.06.027
Linnman C, Coombs 3rd G, Golf DC, Holt DJ (2013) Lack of insula reactivity to aversive stimuli in schizophrenia. Schizophr Res. 143:150-157. https://doi.org/10.1016/j.schres.2012.10.038
Mai JK and Assheuer JK (1999) Atlas of the Human Brain. Academic Press, San Diego.
Makris N, Meyer JW, Bates JF, Yeterian EH, Kennedy DN, et al (1999) MRI-Based topographic parcellation of human cerebral white matter and nuclei II. Rationale and applications with systematics of cerebral connectivity. Neuroimage. 9(1):18-45. https://doi.org/10.1006/nimg.1998.0384
Malcolm JG, Shenton ME, Rathi Y (2010) Filtered multitensor tractography. IEEE Trans Med Imaging. 29(9):1664-1675. https://doi.org/10.1109/TMI.2010.2048121
Mazal PP, Haehner A, Hummel T (2016) Relation of the volume of the olfactory bulb to psychophysical measures of olfactory function. Eur Arch Otorhinolaryngol. 273(1):1-7. https://doi.org/10.1007/s00405-014-3325-7
Menelaou G, Persson J, Olofsson JK (2022) Hippocampal subfield volumes and olfactory performance: Emerging longitudinal associations over a 5-year interval. Neuropsychologia. 176:108353. https://doi.org/10.1016/j.neuropsychologia.2022.108353
Misiak MM, Hipolito MS, Ressom HW, Obisesan TO, Manaye KF, et al (2017) Apo E4 Alleles and Impaired Olfaction as Predictors of Alzheimer's Disease. Clin Exp Psychol. 3(4). https://doi.org/10.4172/2471-2701.1000169
Nieuwenhuys R, Voogd J, van Huijzen C (2008) The Human Central Nervous System, 4th ed. Springer, New York.
Noto T, Zhou G, Yang Q, Lane G, Zelano C (2021) Human Primary Olfactory Amygdala Subregions Form Distinct Functional Networks, Suggesting Distinct Olfactory Functions. Front Syst Neurosci. 15:752320. https://doi.org/10.3389/fnsys.2021.752320
O'Donnell LJ, Westin CF (2007) Automatic tractography segmentation using a high-dimensional white matter atlas. IEEE Trans Med Imaging. 26(11):1562-1575. https://doi.org/10.1109/TMI.2007.906785
Ogg MC, Bendahamane M, Fletcher ML (2015) Habituation of glomerular responses in the olfactory bulb following prolonged odor stimulation reflects reduced peripheral input. Front Mol Neurosci. 8:53. https://doi.org/10.3389/fnmol.2015.00053
Okada N, Kasai K, Takahashi T, Suzuki M, Hashimoto R, et al (2014a) Rating scale of handedness for biological psychiatry research among Japanese people. J. Biol.

Psychiatry. 25: 118-119.
Okada N, Kasai K, Takahashi T, Suzuki M, Hashimoto R, et al (2014b) Brief rating scale of socioeconomic status for biological psychiatry research among Japanese people: A scaling based on an educational history. Japanese J. Biol.Psychiatry. 25: 115-117.
Poellinger A, Thomas R, Lio P, Lee A, Makris N, et al (2001) Activation and habituation in olfaction--an fMRI study. Neuroimage. 13(4):547-560. https://doi.org/10.1006/nimg.2000.0713
Price JL (1990) Olfactory system. In The Human Nervous System (ed Paxinos, G.). Academic Press, San Diego, pp 979-998.
Price JL, Slotnick BM, Revial MF (1991) Olfactory projections to the hypothalamus. J Comp Neurol. 306(3):447-461. https://doi.org/10.1002/cne.903060309
Reddy CP, Rathi Y (2016) Joint Multi-Fiber NODDI Parameter Estimation and Tractography Using the Unscented Information Filter. Front Neurosci. 10:166. https://doi.org/10.3389/fnins.2016.00166
Rolls ET, Kringelbach ML, de Araujo IE (2003) Different representations of pleasant and unpleasant odours in the human brain. Eur J Neurosci. 18(3):695-703. https://doi.org/10.1046/j.1460-9568.2003.02779
Sasabayashi D, Itoh H, Nemoto K, Higuchi Y, Akasaki Y, et al (2025) Saturated Fatty Acids and White Matter Microstructure in Individuals With At-risk Mental State. Schizophr Bull. 52(2):sbaf089. https://doi.org/10.1093/schbul/sbaf089
Savic I, Gulyas B (2000) PET shows that odors are processed both ipsilaterally and contralaterally to the stimulated nostril. Neuroreport. 11(13):2861-2866. https://doi.org/10.1097/00001756-200009110-00007
Saygin ZM, Kliemann D, Iglesias JE, van der Kouwe AJW, Boyd E, et al (2017) High-resolution magnetic resonance imaging reveals nuclei of the human amygdala: manual segmentation to automatic atlas. Neuroimage. 155:370-382. https://doi.org/10.1016/j.neuroimage.2017.04.046
Seubert J, Freiherr J, Frasnelli J, Hummel T, Lundström JN, et al (2013) Orbitofrontal cortex and olfactory bulb volume predict distinct aspects of olfactory performance in healthy subjects. Cereb Cortex. 23(10):2448-2456. https://doi.org/10.1093/cercor/bhs230
Sha Z, Pepe A, Schijven D, Carrión-Castillo A, Roe JM, Westerhausen R, et al (2021) Handedness and its genetic influences are associated with structural asymmetries of the cerebral cortex in 31,864 individuals. Proc Natl Acad Sci U S A. 118(47):e2113095118. https://doi.org/10.1073/pnas.2113095118
Simmons A, Matthews SC, Stein MB, Paulus MP (2004) Anticipation of emotionally aversive visual stimuli activates right insula. Neuroreport. 15:2261-2265. https://doi.org/10.1097/00001756-200410050-00024
Smith SM, Jenkinson M, Woolrich MW, Beckmann CF, Behrens TE, et al (2004) Advances in functional and structural MR image analysis and implementation as FSL. Neuroimage. 23 Suppl 1:S208-219. https://doi.org/10.1016/j.neuroimage.2004.07.051
Soudry Y, Lemogne C, Malinvaud D, Consoli SM, Bonfils P (2011) Olfactory system and emotion: common substrates. Eur Ann Otorhinolaryngol Head Neck Dis. 128(1):18-23. https://doi.org/10.1016/j.anorl.2010.09.007
Takahashi T, Itoh H, Nishikawa Y, Higuchi Y, Nakamura M, et al (2015) Possible relation between olfaction and anxiety in healthy subjects. Psychiatry Clin Neurosci. 69(7):431-438. https://doi.org/10.1111/pcn.12277
Takahashi T, Nakamura M, Sasabayashi D, Nishikawa Y, Takayanagi Y, et al (2019)

Association between olfactory sulcus morphology and olfactory functioning in schizophrenia and psychosis high-risk status. Heliyon. 5(10):e02642. https://doi.org/10.1016/j.heliyon.2019.e02642

Vos SB, Viergever MA, Leemans A (2013) Multi-fiber tractography visualizations for diffusion MRI data. PLoS One. 8(11):e81453. https://doi.org/10.1371/journal.pone.0081453

Wassermann D, Makris N, Rathi Y, Shenton M, Kikinis R, et al (2016) The white matter query language: a novel approach for describing human white matter anatomy. Brain Struct Funct. 221(9):4705-4721. https://doi.org/10.1007/s00429-015-1179-4

Yousem DM, Geckle RJ, Bilker WB, Doty RL (1998) Olfactory bulb and tract and temporal lobe volumes. Normative data across decades. Ann N Y Acad Sci. 855:546-555. https://doi.org/10.1111/j.1749-6632.1998.tb10624.x

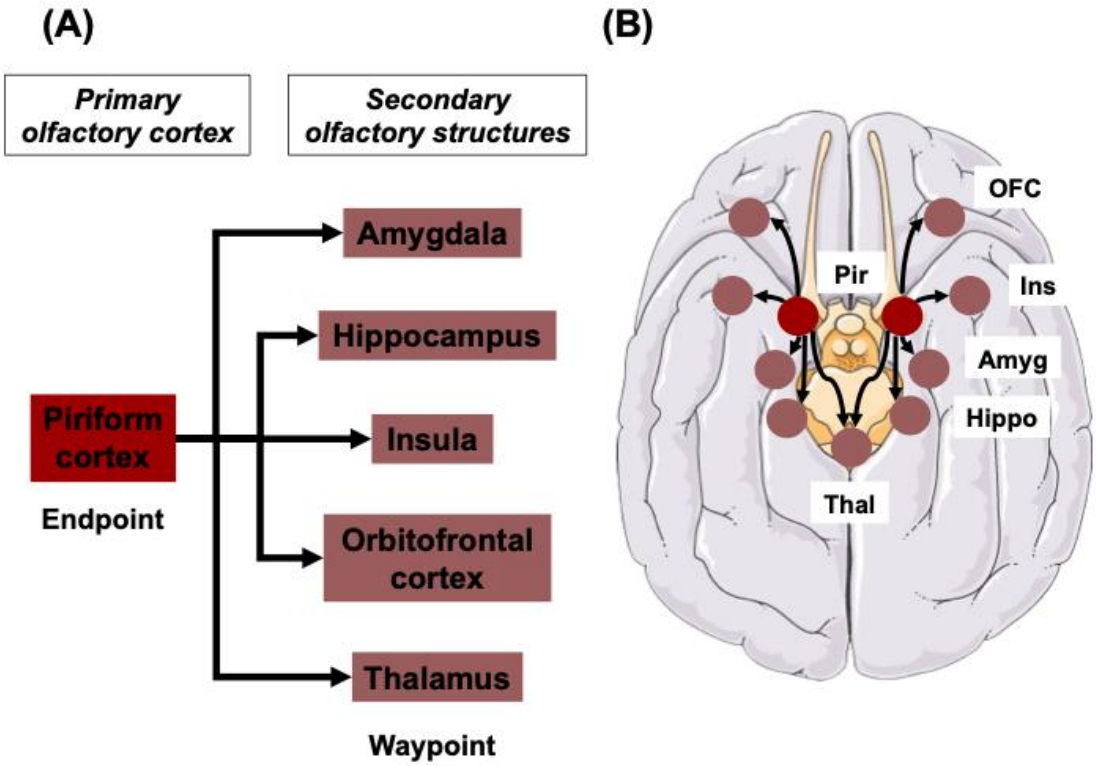
Zhang Y, Zhang J, Oishi K, Faria AV, Jiang H, et al (2010) Atlas-guided tract reconstruction for automated and comprehensive examination of the white matter anatomy. Neuroimage. 52(4):1289-1301. https://doi.org/10.1016/j.neuroimage.2010.05.049

Zhang YJ, Lee JY, Igarashi KM (2024) Circuit dynamics of the olfactory pathway during olfactory learning. Front Neural Circuits. 18:1437575. https://doi.org/10.3389/fncir.2024.1437575

Zhou G, Lane G, Cooper SL, Kahnt T, Zelano C (2019) Characterizing functional pathways of the human olfactory system. Elife. 8:e47177. https://doi.org/10.7554/eLife.47177

Figure legends

Figure 1 Definition of the olfactory pathway for diffusion tractography



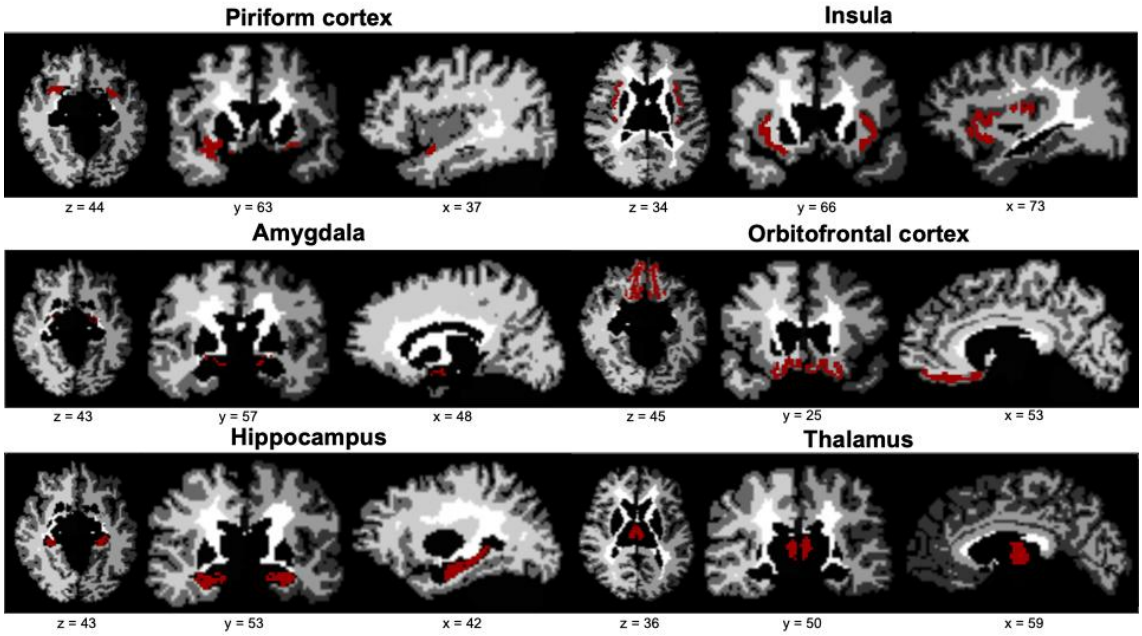
(A) Tracts were defined to originate or terminate in the primary olfactory cortex (endpoints) and to pass through secondary olfactory structures (waypoints).

(B) Axial view from the ventral surface of the brain, illustrating the schematic representation of olfactory pathway according to the criteria defined in (A).

Abbreviation: Amyg, amygdala; Hippo, hippocampus; Ins, insula; OFC, orbitofrontal cortex; Pir, piriform cortex; Thal, thalamus.

Servier Medical Art by Servier, licensed under CC BY 3.0

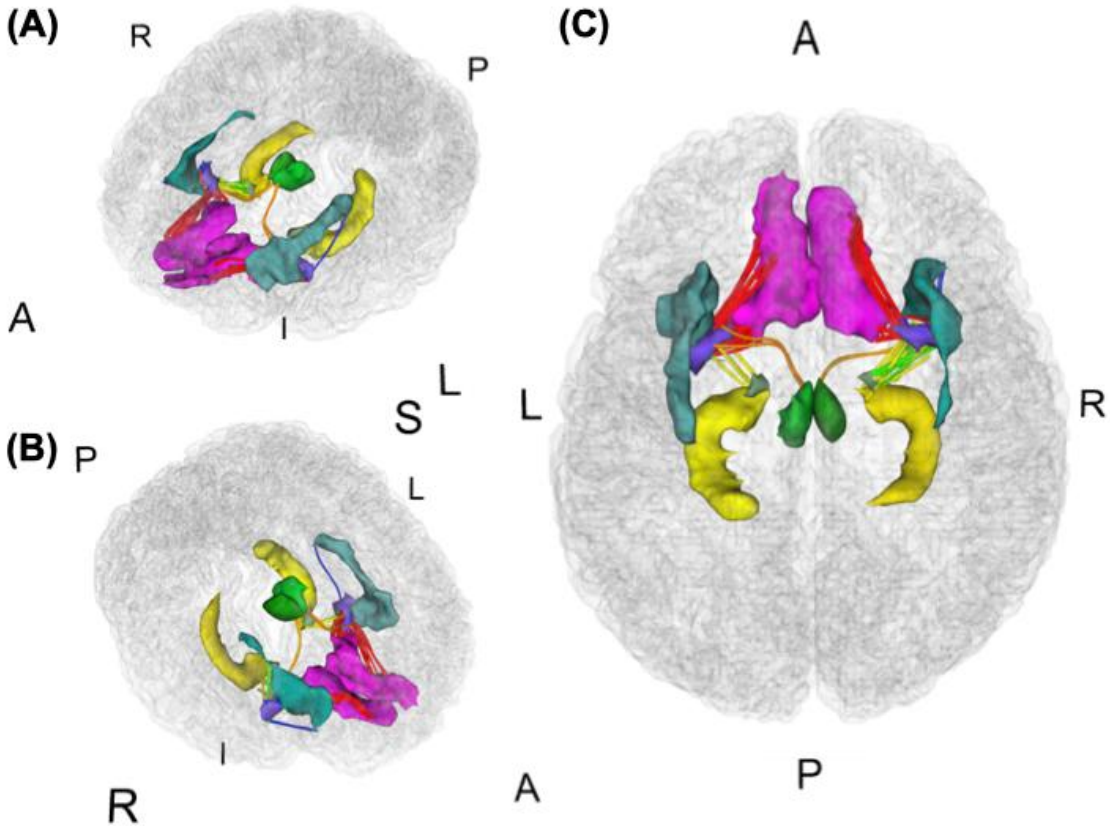
Figure 2 Anatomical definition of primary olfactory cortex and secondary olfactory structures for tractography



Red-colored voxels represent the brain regions comprising the primary olfactory cortex and secondary olfactory structures used for tractography. The figure shows these regions in axial, coronal, and sagittal orientations, with corresponding MNI coordinates indicated below each panel. These definitions were employed to establish endpoints and waypoints for olfactory pathway reconstruction.

Abbreviation: MNI, Montreal Neurological Institute.

Figure 3 Three-dimensional visualization of the olfactory pathway using white matter tractography



Primary olfactory cortex and secondary olfactory structures are colored as follows: piriform cortex (purple), amygdala (desaturated green), hippocampus (yellow), insula (teal), orbitofrontal cortex (magenta), and thalamus (bright green).

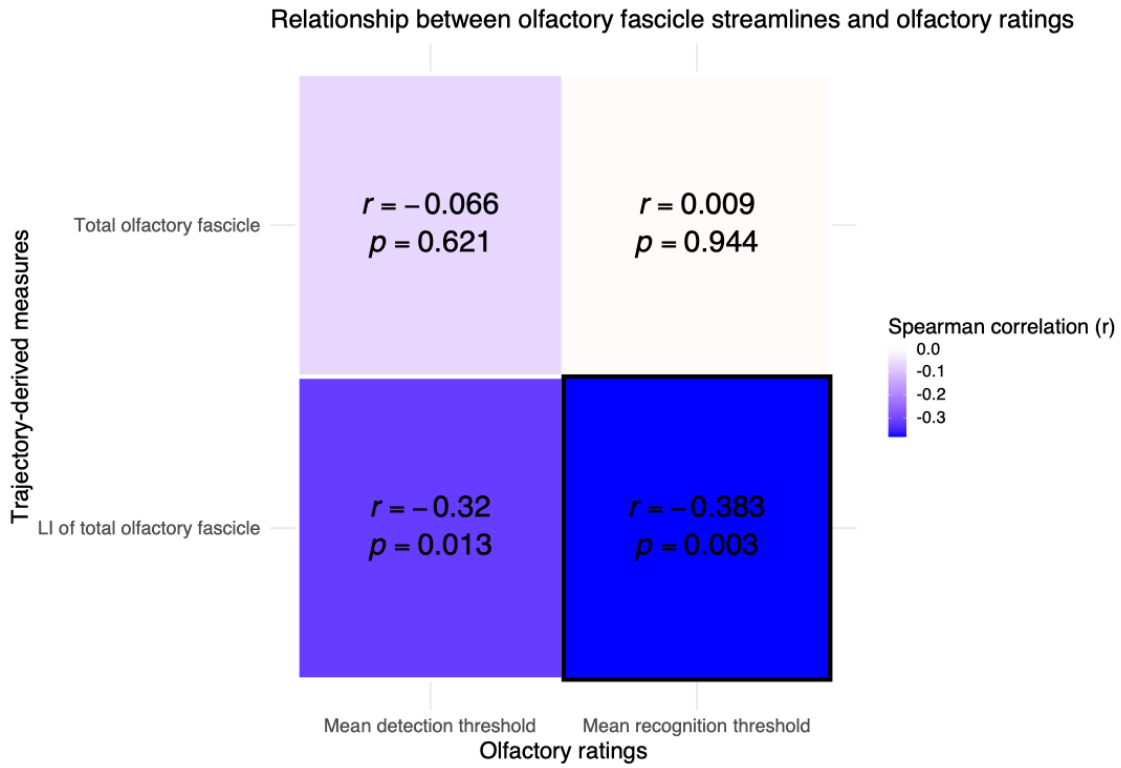
Reconstructed olfactory streamlines are displayed with distinct colors for each fascicle: olfactory amygdala fascicle (bright green), olfactory hippocampus fascicle (yellow), olfactory insula fascicle (blue), olfactory orbitofrontal cortex fascicle (red), and olfactory thalamus fascicle (orange).

Panels show different perspectives: (A) left anterior oblique, (B) right anterior oblique, and (C) superior view.

Three-dimensional axis labels indicate: A = anterior, P = posterior, S = superior, R =

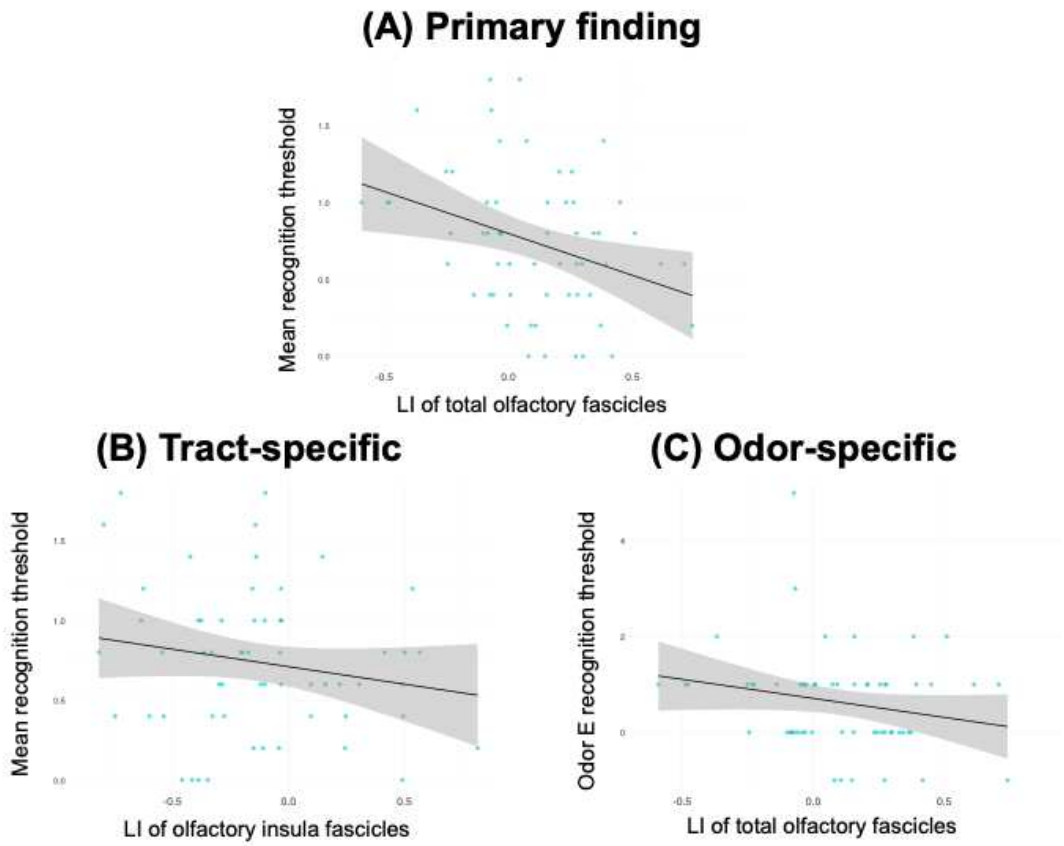
right, and L = left.

Figure 4 Relationship between olfactory fascicle streamlines and olfactory function



Spearman correlation between two trajectory-derived measures of the olfactory fascicle—Total olfactory fascicle (total number of streamlines) and LI of total olfactory fascicle (Laterality Index)—and olfactory detection and recognition thresholds. Each cell shows the correlation coefficient (*r*, top) and the associated *p*-value (bottom). Cells that are significant after Bonferroni correction are highlighted with a black border. Color shading indicates the direction and magnitude of the correlation (blue: negative correlation; white: weak or no correlation).

Figure 5 Scatter plots of olfactory fascicle streamlines and olfactory ratings



(A) Primary finding: Relationship between LI of the number of streamlines in the total olfactory fascicle and mean recognition threshold

(B) Tract-specific: Relationship between LI of the number of streamlines in the olfactory insula fascicle and mean recognition threshold

(C) Odor-specific: Relationship between LI of the number of streamlines in the total olfactory fascicle and odor E recognition threshold

Abbreviation: LI, Laterality Index

Table 1. Characteristics of study participants by sex group

	Whole (n = 129)	Male (n = 65)	Female (n = 64)	Sex difference (Male *vs.* Female) Test Statistic	P Value
Age, years, mean (SD)	25.8 (3.7)	27.2 (3.8)	24.4 (3.0)	F(1,128) = 21.850	$p < 0.001$*
Handedness, right/mixed/left, No.	95/26/8	47/12/6	48/14/2	$\chi^2(2) = 2.157$	$p = 0.340$
Socioeconomic status, mean (SD)	6.3 (0.9)	6.5 (0.7)	6.0 (0.9)	F(1,128) = 12.530	$p < 0.001$*
Parental socioeconomic status, mean (SD)	6.0 (0.9)	6.2 (0.8)	5.8 (1.0)	F(1,129) = 6.830	$p = 0.010$*
Cigarette smoker, No. (%)	5 (3.9)	3 (4.6)	2 (3.1)	$\chi^2(1) = 0.192$	$p = 0.661$
Intracranial volume, cm^3, mean (SD)	1004.2 (84.4)	1046.6 (68.7)	961.1 (77.2)	F(1,128) = 44.153	$p < 0.001$*
Bilateral Piriform volume, cm^3, mean (SD)	1.8 (0.3)	1.9 (0.2)	1.6 (0.2)	F(1,128) = 51.493	$p < 0.001$*
	Whole (n = 59)	Male (n = 32)	Female (n = 27)	Sex difference (Male *vs.* Female) Test Statistic	P Value
Odor detection threshold, mean (SD)					
Odor A (rose)	-0.1 (0.9)	-0.1 (0.9)	-0.2 (0.8)	MWU = 481.5	$p = 0.424$
Odor B (caramel)	0.1 (0.6)	0.1 (0.6)	0.0 (0.6)	MWU = 478.0	$p = 0.388$
Odor C (rotten food or sweaty clothes)	0.3 (0.7)	0.1 (0.7)	0.5 (0.7)	MWU = 303.0	$p = 0.032$
Odor D (sweet fruit)	0.3 (0.8)	0.2 (0.9)	0.5 (0.6)	MWU = 338.5	$p = 0.123$
Odor E (fecal material)	-0.3 (0.6)	-0.2 (0.6)	-0.5 (0.6)	MWU = 532.5	$p = 0.083$
Mean	0.0 (0.4)	0.3 (0.5)	0.5 (0.4)	MWU = 439.0	$p = 0.914$
Odor recognition threshold, mean (SD)					
Odor A (rose)	0.9 (0.8)	1.1 (0.8)	0.7 (0.8)	MWU = 540.0	$p = 0.075$
Odor B (caramel)	0.6 (0.6)	0.7 (0.6)	0.4 (0.5)	MWU = 514.5	$p = 0.157$
Odor C (rotten food or sweaty clothes)	0.6 (0.6)	0.5 (0.6)	0.8 (0.5)	MWU = 314.0	$p = 0.034$
Odor D (sweet fruit)	1.0 (0.6)	1.1 (0.7)	0.9 (0.6)	MWU = 492.0	$p = 0.294$
Odor E (fecal material)	0.6 (1.0)	0.8 (0.9)	0.4 (1.2)	MWU = 555.5	$p = 0.045$
Mean	0.7 (0.5)	0.8 (0.4)	0.6 (0.4)	MWU = 533.0	$p = 0.121$
Subjects with olfactory deficits, No. (%)	11 (18.6)	7 (21.9)	4 (14.8)	$\chi^2(1) = 0.481$	$p = 0.488$
STAI trait	40.8 (8.3)	39.1 (7.4)	42.9 (8.9)	F(1,58) = 3.257	$p = 0.076$
STAI state	37.1 (6.1)	35.8 (5.9)	38.8 (6.1)	F(1,58) = 3.743	$p = 0.058$

Abbreviation: STAI, State-Trait Anxiety Inventory

* denotes statistical significance

Table 2. Comparison of the number of streamlines in the olfactory fascicle between left and right hemispheres

Primary analysis	Bilateral		Left		Right		Hemisphere differences (Left *vs.* Right)	
	Mean	SD	Mean	SD	Mean	SD	t	*p*
Total olfactory fascicle	231.50	108.05	137.78	88.43	93.73	53.52	5.081	1.0×10^{-6} *
Post-hoc analyses	Bilateral		Left		Right		Hemisphere differences (Left *vs.* Right)	
	Mean	SD	Mean	SD	Mean	SD	t	*p*
Olfactory amygdala fascicle	18.24	13.16	8.06	7.99	11.73	10.11	-3.286	0.001*
Olfactory hippocampus fascicle	15.18	16.33	7.68	11.80	8.80	10.71	-0.96	0.34
Olfactory thalamus fascicle	4.28	4.20	2.47	2.97	3.42	3.50	-1.854	0.07
Olfactory insula fascicle	89.06	58.11	43.77	37.65	45.64	39.00	-0.464	0.643
Olfactory OFC fascicle	133.31	76.40	96.51	73.71	37.09	24.36	9.168	1.1×10^{-15} *

Abbreviation: OFC, orbitofrontal cortex

* denotes statistical significance (after Bonferroni correction in Post-hoc analyses)

Table 3. LI of the number of streamlines in the olfactory fascicles

	Mean	SD
Total olfactory fascicle	0.140	0.338
Olfactory amygdala fascicle	-0.169	0.488
Olfactory hippocampus fascicle	-0.046	0.522
Olfactory thalamus fascicle	-0.163	0.408
Olfactory insula fascicle	-0.050	0.428
Olfactory OFC fascicle	0.313	0.390

Abbreviation: LI, Laterality Index

Table 4. Comparison of the number of streamlines in the olfactory fascicle between male and female

Primary analysis	Male (n = 65)		Female (n = 64)		Sex differences (Male *vs.* Female)	
	Mean	SD	Mean	SD	F	p
Total olfactory fascicle	262.97	116.46	199.55	88.78	7.548	0.007*
Post-hoc analyses	Male (n = 65)		Female (n = 64)		Sex differences (Male *vs.* Female)	
	Mean	SD	Mean	SD	F	p
Olfactory amygdala fascicle	20.38	14.15	16.06	11.79	4.994	0.027
Olfactory hippocampus fascicle	14.79	16.63	15.58	16.14	0.038	0.845
Olfactory thalamus fascicle	3.55	3.21	5.10	4.99	3.196	0.077
Olfactory insula fascicle	100.17	67.74	77.78	44.07	2.451	0.120
Olfactory OFC fascicle	154.32	82.10	111.97	63.97	9.289	0.003*

* denotes statistical significance (after Bonferroni correction in Post-hoc analyses)

Supplementary Files

This is a list of supplementary files associated with this preprint. Click to download.

- SupplementaryInformationV3.pdf